10942 *Inorg. Chem.* **2009**, *48*, 10942–10953
DOI: 10.1021/ic900330q

Inorganic Chemistry
Article

Reduction of Ferricytochrome *c* Catalyzed by Optically Active Chromium(III) Complexes

Ulrich Scholten,*,† Céline Diserens,† Helen Stoeckli-Evans,‡ Klaus Bernauer,*,§ Michel Meyer,*,∥ Ludovic Stuppfler,∥ and Dominique Lucas∥

†*Ecole d'Ingénieurs et d'Architectes de Fribourg, Département des Technologies Industrielles, Boulevard de Pérolles 80, Case Postale 32, 1705 Fribourg, Switzerland,* ‡*Université de Neuchâtel, Institut de Physique, Rue Emile-Argand, 2009 Neuchâtel, Switzerland,* §*Université de Neuchâtel, Institut de Chimie, Avenue de Bellevaux 51, Case Postale 158, 2009 Neuchâtel, Switzerland, and* ∥*Institut de Chimie Moléculaire de l'Université de Bourgogne (ICMUB), UMR 5260 du CNRS, 9 Avenue Alain Savary, Boîte Postale 47870, 21078 Dijon Cedex, France*

Received February 18, 2009

The reduction rates of horse heart ferricytochrome *c* by amalgamated zinc or by electrolysis at fixed potential on a mercury pool as the cathode have been measured in a buffered solution at pH 7.5 by absorption spectrophotometry. In both cases, the reaction was strongly accelerated by the presence of the optically active complexes Λ-$[Cr^{III}((S,S)\text{-promp})H_2O]^+$ (H_2promp = *N*,*N*′-[(pyridine-2,6-diyl)bis(methylene)]-bis[(*S*)-proline]), Δ-$[Cr^{III}((R,R)\text{-alamp})H_2O]^+$ (H_2alamp = *N*,*N*′-[(pyridine-2,6-diyl)bis(methylene)]-bis[(*R*)-alanine]) and Λ-$[Cr^{III}((S,S)\text{-alamp})(H_2O)_2]^+$. These were shown to undergo reversible one-electron reduction to the corresponding labile chromium(II) species by cyclic voltammetry (CV), although the diaquo Λ-$[Cr^{III}((S,S)\text{-alamp})(H_2O)_2]^+$ compound behaved differently than the two others. The cyclic voltammogram evidenced a strong catalytic reduction wave below −1.1 V/SHE overlapping with the Cr^{3+}/Cr^{2+} couple, which has been attributed to the catalytic reduction of hydroxonium ions to molecular hydrogen. Although stable in the second time range as demonstrated by CV, the chromium(II) complexes exist in solution only as short-lived species in the absence of protein and are rapidly reoxidized to the initial trivalent state, thus preventing their isolation even under anaerobic conditions. However, their lifetime was found to be long enough to catalyze the reduction of the ferric heme moiety of cytochrome *c* according to an electron-transfer-mediated reaction. Both chemical and electrochemical processes were found to follow zero-order kinetics. It could therefore be safely concluded that the rate-determining step is associated to the electron transfer from transient chromium(II) complexes to the protein and not to the in situ generation of the metallic reducing agent.

Introduction

Optically active pyridyldiaminocarboxylate ligands synthesized from D- or L-amino acids, like the proline and alanine derivatives noted $promp^{2-}$ and $alamp^{2-}$ shown in Figure 1, are known to react stereospecifically with both inert as well as labile transition metal ions to form complexes exhibiting definite chirality (i.e., ligands with *R* configuration on both asymmetric carbon atoms afford complexes possessing a Δ helicity).[1−3] These metal complexes have been shown to be useful stereoselective probes in electron transfer reactions involving various metalloenzymes.[4−9] Chiral recognition of the spinach plastocyanine surface by a reducing agent could be demonstrated in that way using both enantiomers of $[Fe^{II}(alamp)]$,[4] while genetic modifications further enabled to identify the residue (Leu-12) responsible for the stereoselectivity.[10] However, the most efficient strategy relies on the proper choice of a labile low-valent

*To whom correspondence should be addressed. E-mail: ulrich.scholten@hefr.ch (U.S.), klaus.bernauer@unine.ch (K.B.), michel.meyer@u-bourgogne.fr (M.M.).

(1) Bernauer, K.; Pousaz, P. *Helv. Chim. Acta* **1984**, *67*, 796–803.
(2) Bernauer, K.; Stoeckli-Evans, H.; Hugi-Cleary, D.; Hilgers, H. J.; Abd-el-Khalek, H.; Porret, J.; Sauvain, J. J. *Helv. Chim. Acta* **1992**, *75*, 2327–2339.
(3) Bernauer, K.; Pousaz, P.; Porret, J.; Jeanguenat, A. *Helv. Chim. Acta* **1988**, *71*, 1339–1348.
(4) Bernauer, K.; Sauvain, J. J. *J. Chem. Soc., Chem. Commun.* **1988**, 353–354.
(5) Bernauer, K.; Verardo, L. *Angew. Chem., Int. Ed. Engl.* **1996**, *35*, 1716–1717.
(6) Bernauer, K.; Ghizdavu, S.; Verardo, L. *Coord. Chem. Rev.* **1999**, *190−192*, 357–369.
(7) Sasaki, S.; Nishijima, Y.; Koga, H.; Ohkubo, K. *Inorg. Chem.* **1989**, *28*, 4061–4063.
(8) Sasaki, S.; Nishijima, Y.; Koga, H.; Ohkubo, K. *J. Chem. Soc., Dalton Trans.* **1991**, 1143–1148.
(9) Bernauer, K.; Jauslin, P. *Chimia* **1993**, *47*, 218–220.
(10) Bernauer, K.; Schürmann, P.; Nusbaumer, C.; Verardo, L.; Ghizdavu, S. *Pure Appl. Chem.* **1998**, *70*, 985–991.

 Published on Web 10/28/2009

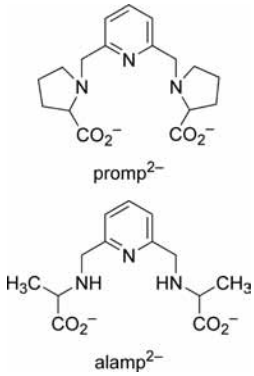

Figure 1. Molecular formula of both ligands considered in this work.

redox-active cation as reactant (e.g., Co^{2+}, Cr^{2+}), which becomes inert in the higher oxidation state (e.g., Co^{3+}, Cr^{3+}) and thus remains coordinated to the electron acceptor in case of an inner-sphere electron-transfer mechanism or stays in solution for an outer-sphere process. Provided the chirality of the metal complex is imposed by the fixed configuration of the ligand, preventing thereby both racemization and inversion, this approach allowed one to unravel by circular dichroism (CD) spectroscopy both the stereoselectivity of the reaction and the nature of the coordinating group at which the electron transfer has taken place.

Following that approach, the reduction mechanisms of the blue copper proteins plastocyanin[5] and azurin[10] or the hemoprotein cytochrome *c*[11] by the enantiomerically pure Δ- and Λ-[Co^{II}(alamp)] complexes have been investigated. The stereoselectivity of the electron-transfer reaction was found to be associated with marked differences in the activation parameters, suggesting either a chiral discrimination in the transition state of the entering complexes by the same site of the protein or, alternatively, the selection by each optical antipode of its own interaction site. For all systems studied so far, the enantiomer showing the lowest activation enthalpy is disadvantaged by a more negative activation entropy so that the stereoselectivity is strongly temperature dependent and can even be inversed in specific temperature ranges. Of relevance from a mechanistic point of view, significant enantioselective binding could be detected by the CD spectroscopic signature of the inert cobalt(III) adducts that remained covalently attached to the biological material after dialysis of the reaction products. It was thereby demonstrated that the imidazole side chain of histidines could act as a bridge in the bimolecular inner-sphere electron transfer (His-87 in plastocyanine, His-83 in azurin, His-26 or 33 in cytochrome *c*).[6,11] Regardless of the metalloprotein under investigation, the right- and left-handed [M^{II}(promp)] complexes systematically give rise to much lower kinetic stereoselectivities due to the less differentiated activation parameters. The steric exclusion due to the hindrance of the proline units in [M^{II}(promp)] complexes, together with their inability to form hydrogen bonds via the coordinated amino groups, are plausible explanations for the less efficient stereognostic interactions with the protein surface.[10] Fixation experiments have confirmed this trend: so far azurin is the only protein for which covalent binding could be detected after reduction with [Co^{II}(promp)], although in a considerably smaller extent in comparison with [Co^{II}(alamp)].[6]

Unfortunately, the electrochemical potential of cobalt(II) complexes restricts the application of this technique to metalloproteins exhibiting rather positive electrochemical potentials like blue copper proteins or cytochrome *c*. It seemed therefore interesting to explore the possibility to use chromium complexes as one-electron reducing agents, possessing largely negative redox potentials and containing a metal center forming, like cobalt, labile complexes in the lower oxidation state but inert species in the higher one. Indeed, chromium(II) was one of the first inorganic compounds used for reducing cytochrome *c*. Reduction by aqueous Cr^{2+} led to roughly 50% binding of chromium to the protein, while uptake became almost complete when a Cr^{2+}−phosphate complex was used as the reducing agent.[12] In that case, it was not possible to identify the amino acid residues that were involved as bridging groups in the electron transfer, but protein digestion yielded a peptide fragment containing iron, chromium, and phosphate in a nearly 1:1:1 ratio. Dawson et al. studied the reduction kinetics by chromous ions of several metalloproteins, including *Rhus* laccase, the blue copper proteins plastocyanin and stellacyanin, as well as cytochrome *c*.[13] The reduction of cytochrome *c* by Cr^{2+} follows a simple second-order rate law, while a two-step reduction mechanism was found for its derivative carboxymethylated at the heme-linked methionine. In the latter case, the intermediate was attributed to a low spin ferrous complex.[14] The catalytic activity of anions on the reduction of cytochrome *c* by chromium(II) has been studied over a large pH range; the mechanism of the reaction has been discussed taking into account the various species involved and the chromium(III) products formed during the reaction.[15,16] By using solutions of radioactively labeled Cr^{2+}, Grimes et al. showed that the reduction of ferricytochrome *c* in slightly acidic solution led to intramolecular cross-linking of the peptide chain, chromium(III) being bound to tyrosine-67 and to asparagine-52.[17] Accordingly, the authors suggest that tyrosine-67 should be involved in the electron transfer. Similarly, the electron-transfer mediated binding of chromium(III) enabled to identify the carboxylate side chains of the amino acids 42 to 45 of plastocyanin as possible electron transfer sites.[18] The neighborhood of tyrosine-83 was thought to be indicative for the participation of the latter in the electron transfer pathway.

Besides complexes with simple anions like phosphate, chloride, or thiocyanate, only very few examples of chromium(II) complexes have been employed as reducing agents of metalloproteins or model compounds. [Cr^{II}(edta)]$^{2-}$ was used as a reductant in the reaction with a model Fe−S cluster,[19] whereas the macrocyclic complex [Cr^{II}([15]aneN$_4$)(H$_2$O)$_2$]$^{2+}$ allowed the distinction between an inner- and outer-sphere electron

(11) Scholten, U.; Castillejo Merchán, A.; Bernauer, K. *J. R. Soc. Interface* **2005**, *2*, 109–112.

(12) Kowalski, A. *J. Biol. Chem.* **1969**, *244*, 6619–6625.
(13) Dawson, J. W.; Gray, H. B.; Holwerda, R. A.; Westhead, E. W. *Proc. Natl. Acad. Sci. U.S.A.* **1972**, *69*, 30–33.
(14) Brittain, T.; Wilson, M. T.; Greenwood, C. *Biochem. J.* **1974**, *141*, 455–461.
(15) Yandell, J. K.; Fay, D. P.; Sutin, N. *J. Am. Chem. Soc.* **1973**, *95*, 1131–1137.
(16) Przystas, T. J.; Sutin, N. *Inorg. Chem.* **1975**, *14*, 2103–2110.
(17) Grimes, C. J.; Piszkiewicz, D.; Fleischer, E. B. *Proc. Natl. Acad. Sci. U.S.A.* **1974**, *71*, 1408–1412.
(18) Farver, O.; Pecht, I. *Proc. Natl. Acad. Sci. U.S.A.* **1981**, *78*, 4190–4193.
(19) Henderson, R. A.; Sykes, A. G. *Inorg. Chem.* **1980**, *19*, 3103–3105.

transfer mechanism involving [4Fe−4S] and [2Fe−2S] ferredoxins.[20−23] Nevertheless, the reduction with an optically active chromium(II) complex has not been mentioned thus far. We report herein the first application of chiral chromium(II) complexes incorporating the optically active ligands promp^{2-} and alamp^{2-} (Figure 1) for the reduction of a metalloprotein. Indeed, these complexes should be enantiomerically pure and labile toward ligand exchange, while exhibiting a strongly negative reduction potential. Altogether, these suited properties might most likely confer them the status of a general-purpose reducing agent of metalloenzymes, including those possessing negative reduction potentials, such as plant ferredoxin. En route, we have chosen to study first the reduction of horse-heart ferricytochrome *c*, which appeared as the ideal system for validation purposes.

Experimental Section

Safety Note. *Although no problems were experienced in handling perchlorate compounds, these salts when combined with organic ligands are potentially explosive and should be manipulated with care and used only in very small quantities.*

Physical and Spectroscopic Measurements. Circular dichroism (CD) spectra were recorded on a J-715 (Jasco) single beam spectropolarimeter. UV−vis spectra were collected on a Lamda 12 (Perkin-Elmer) spectrophotometer. Positive mode high-resolution electrospray-ionization mass spectra (HR-ESI-MS) of complexes dissolved in a 50/50 v/v methanol−water mixture or pure ethanol ($c = 10^{-5}$ M) were obtained on a FTMS BioAPEX II (Bruker) or a microTOF-Q (Bruker) instrument, respectively. Cyclic voltammograms were recorded with a Polarograph 694 VA (Metrohm) using a hanging mercury drop as the working electrode, a platinum wire as the auxiliary electrode, and an Ag/AgCl reference electrode. No ohmic drop compensation was applied. All potential values are referenced to the standard hydrogen electrode (SHE, correction applied for potentials measured vs Ag/AgCl/KCl 3M: + 0.19 V). Coulometric studies of pure complexes ($c = 10^{-3}$ M) in the Tris/HCl buffer (pH = 7.5; $I = 0.1$ M) were performed on a stirred mercury pool using a gastight three-electrode cell equipped with a KCl-saturated calomel (SCE) reference electrode (XR110 from Radiometer) separated from the bulk by a sintered-glass bridge filled with the buffer solution and a platinum wire as the counter electrode. An Amel 552 potentiostat was used to apply a fixed potential of −1.4 V/SCE (−1.16 V/SHE), whereas the charge was monitored with a Tacussel IG5-N integrator. For H_2 identification, a 2.25×10^{-3} M test solution of $PdCl_2$ in water was prepared in an independent flask. At the end of the electrolysis, the gases contained in the headspace of the cell were transferred into the flask containing the $PdCl_2$ solution by means of a gastight syringe. Precipitation of palladium black particles after a few minutes attested the generation of H_2 during the electrolysis of Λ-[Cr^{III}((*S*,*S*)-alamp)(H_2O)$_2$]ClO_4 (a positive test was also obtained for the gases evolved during the electrolysis of acidic water at a large area platinum electrode).[24,25] In contrast, no Pd particles formed in the test solution when either Tris/HCl buffer or a Δ-[Cr^{III}((*R*,*R*)-alamp)(H_2O)]ClO_4 solution was electrolyzed.

Chemicals. Horse heart ferricytochrome *c* 95% from Fluka was used without further purification. Ligands were synthesized according to previously published procedures.[1,3] All other reagents were of analytical grade. The pH 4.5 buffer solutions were prepared by mixing a sodium acetate solution with concentrated acetic acid and then diluted to the desired ionic strength. Buffer solutions at pH values comprised between 7 and 9 (Tris/HCl) have been prepared from 1.0 M hydrochloric acid (Merck, Titrisol) and solid tris(hydroxymethyl)aminomethane (Tris) and have been diluted to the desired ionic strength. pH 9 buffer at ionic strength $I = 0.2$ M has been prepared by mixing 0.15 M NaCl, 1.0 M hydrochloric acid, and solid Tris.

Preparation of Chromium(III) Complexes. Chromium complexes were prepared in a way analogous to that described in previous publications for the corresponding cobalt(III) compounds.[2]

Λ-[Cr^{III}((*S*,*S*)-promp)H_2O]ClO_4. *N*,*N*′-[(Pyridine-2,6-diyl)bis(methylene)]-bis[(*S*)-proline] (H_2(*S*,*S*)-promp, 16.2 g, 0.04 mol) and $KCr(SO_4)_2 \cdot 12H_2O$ (21.0 g, 0.042 mol) were dissolved in water (250 mL). The solution was maintained at 60 °C and pH 5 by addition of 5 M NaOH as long as the intensity of the CD signal at 500 nm increased. The deep violet solution was concentrated nearly to dryness, and part of chromium(III) in excess was precipitated as hydroxide by the addition of some methanol and then removed by filtration. The filtrate was diluted to 500 mL and purified by cation exchange chromatography (SP Sephadex C-25 in the Na^+ form; column length, 30 cm; bed volume, 700 mL). The column was washed with 5×10^{-4} M acetic acid until the conductivity of the effluent was equal to that of the eluent. The neutral Λ-[Cr^{III}((*S*,*S*)-promp)OH] was displaced by 0.1 M ammonia whereas the residual Cr^{3+} remained fixed on the column. The concentrated fractions containing Λ-[Cr^{III}((*S*,*S*)-promp)OH] were further purified by ion exclusion chromatography (Sephadex G-10; column length, 130 cm; bed volume, 2000 mL). The resulting red and blue bands, corresponding to Λ-[Cr^{III}((*S*,*S*)-promp)H_2O]$^+$ and Λ-[Cr^{III}((*S*,*S*)-promp)OH], were combined, acidified to pH 4 by diluted acetic acid, and fixed again on a cationic ion-exchanger (SP Sephadex C-25 in the Na^+ form; column length, 30 cm; bed volume, 300 mL). The resin was washed with 5×10^{-4} M acetic acid. The Λ-[Cr^{III}((*S*,*S*)-promp)H_2O]$^+$ complex was eluted with 0.5% $NaClO_4$ acidified to pH 4 by 1% $HClO_4$. The concentrated fractions were neutralized and purified by ion exclusion chromatography. The salt-free fractions containing the aqua- and hydroxo-complexes were concentrated and acidified to pH 4 by 1% $HClO_4$. After 7 days, dark violet plates crystallized from the solution at room temperature. Potentiometric titration (H_2O, $I = 0.1$ M KNO_3, $T = 295(3)$ K, $c_0 = 8 \times 10^{-3}$ M): pK_a = 6.85. (+) HR-ESI-MS: m/z = 401.10 [Cr(L)(H_2O)]$^+$ (L = $C_{17}H_{21}N_3O_4^{2-}$). Anal. Calcd (found) for $C_{17}H_{23}ClCrN_3O_9$: C, 40.77 (40.77); H, 4.63 (4.56); N, 8.39 (8.40); Cl, 7.08 (7.11).

Λ-[Cr^{III}((*S*,*S*)-alamp)(H_2O)$_2$]$ClO_4 \cdot H_2O$. *N*,*N*′-[(Pyridine-2,6-diyl)bis(methylene)]-bis[(*S*)-alanine] (H_2(*S*,*S*)-alamp, 1.00 g, 3.55 mmol) and $CrCl_3 \cdot 6H_2O$ (1.00 g, 3.75 mmol) were dissolved separately in water (50 mL). Both solutions were mixed under stirring, and the mixture was brought to pH 5 with 2 M NaOH affording a $Cr(OH)_3$ precipitate. The pH drop was compensated by the addition of NaOH. At that stage, the mixture was heated to 60−70 °C, while the color of the mixture turned slowly to violet. As the ligand reacts with $Cr(OH)_3$, the pH value tends to increase and it was kept at 5 by the addition of HCl during ∼20 h at 60−70 °C under gentle stirring. NaOH was finally added to raise the pH up to 10 while stirring was maintained during one more hour. The mixture was cooled, and the remaining $Cr(OH)_3$ was separated by filtration. $HClO_4$ was added to the filtrate up to pH ≈ 3, the solution was diluted to ∼500 mL and fixed on a cation exchanging resin (SP Sephadex C-25 in the Na^+ form; column length, 120 cm; bed volume,

(20) Adzamli, I. K.; Henderson, R. A.; Ong, H.; Sykes, A. G.; Cammack, R.; Rao, K. K. *Biochem. Biophys. Res. Commun.* **1982**, *105*, 1582–1589.
(21) Adzamli, I. K.; Henderson, R. A.; Sinclair-Day, J. D.; Sykes, A. G. *Inorg. Chem.* **1984**, *23*, 3069–3073.
(22) Im, S. C.; Kohzuma, T.; McFarlane, W.; Gaillard, J.; Sykes, A. G. *Inorg. Chem.* **1997**, *36*, 1388–1396.
(23) Im, S. C.; Worrall, J. A. R.; Liu, G.; Aliverti, A.; Zanetti, G.; Luchinat, C.; Bertini, I.; Sykes, A. G. *Inorg. Chem.* **2000**, *39*, 1755–1764.
(24) Burns, D. T.; Townshend, A.; Carter, A. H. *Inorganic Reaction Chemistry*; Halsted: New York, 1981; Vol. *2*, p 191.
(25) Meilleur, D.; Rivard, D.; Harvey, P. D.; Gauthron, I.; Lucas, D.; Mugnier, Y. *Inorg. Chem.* **2000**, *39*, 2909–2914.

1500 mL). The column was washed with water, and the complex eluted as the neutral species with $NaHCO_3/Na_2CO_3$ buffer (0.05 M; pH = 10). The eluate was brought to pH = 3−4 by addition of $HClO_4$ and concentrated at about 50 °C under reduced pressure. The resulting solution was introduced carefully on the top of a column for ion exclusion chromatography (Sephadex G-10; column length, 130 cm; bed volume, 2000 mL) and eluted with water that was acidified with some drops of concentrated acetic acid. The colored, salt-free fractions (controlled by conductivity measurements) were collected and evaporated almost to dryness at low temperature and pressure. The product was dried over H_2SO_4 under reduced pressure. Yield: 0.55 g, 32%. (+) HR-ESI-MS: m/z = 331.07 $[Cr(L)]^+$, 349.08 $[Cr(L)H_2O]^+$, 679.14 $[Cr_2(L)_2OH]^+$, 693.16 $[Cr_2(L)_2(CH_3O)]^+$, 725.19 $[Cr_2(L)_2(CH_3O)_2 + H]^+$, 747.17 $[Cr_2(L)_2(CH_3O)_2 + Na]^+$ ($L = C_{13}H_{17}N_3O_4^{2-}$). Anal. Calcd (found) for $C_{13}H_{23}ClCrN_3O_{11}$: C, 32.21 (32.03); H, 4.78 (5.10); N, 8.67 (8.60).

Δ-[Cr^{III}((*R*,*R*)-alamp)H$_2$O]ClO$_4$·0.5H$_2$O. The complex was prepared according to the same procedure as mentioned above although with slight modifications: the pH of the solution was kept below 7 during the whole process, while a 1% $NaClO_4$ solution slightly acidified with some drops of concentrated acetic acid was used to elute the complex on the cationic ion exchanger instead of the $NaHCO_3/Na_2CO_3$ buffer. Potentiometric titration (MeOH/H_2O 50/50 v/v, I = 0.1 M $NaClO_4$, T = 298.2(2) K, $c_0 = 10^{-3}$ M): pK_a = 6.54(2). (+) HR-ESI-MS: m/z = 331.08 $[Cr(L)]^+$, 349.09 $[Cr(L)H_2O]^+$, 693.16 $[Cr_2(L)_2(CH_3O)]^+$ ($L = C_{13}H_{17}N_3O_4^{2-}$). Anal. Calcd (found) for $C_{13}H_{20}ClCrN_3O_{9.5}$: C, 34.11 (34.10); H, 4.40 (4.28); N, 9.17 (9.20).

X-ray Crystallographic Data Collection. Purple single-crystals were obtained by slow evaporation from an aqueous solution of the Λ-[Cr^{III}((*S*,*S*)-promp)H$_2$O]ClO$_4$ complex. A high-quality specimen of rodlike shape (0.50 × 0.30 × 0.13 mm^3) was selected for the X-ray diffraction experiment. Data were collected at 223(2) K on a Stoe Image Plate Diffraction system using Mo Kα graphite-monochromated radiation (λ = 0.710 73 Å). A total number of 7882 reflections were collected over the θ range 3.49−25.87° and merged into 3625 independent reflections (R_{int} = 0.0231). The structure was solved by direct methods using the program SHELXS-97.[26] The refinement and all further calculations were carried out using SHELXL-97.[26] H-atoms were included in calculated positions and treated as riding atoms using SHELXL-97 default parameters. The non-H atoms were refined anisotropically using weighted full-matrix least-squares on F^2. Multiscan absorption corrections were applied. The coordinates correspond to the absolute structure of the molecule in the crystal. The value of the Flack parameter was −0.003(15) at the final stages of refinement. The two proline rings were found to be disordered with two possible positions for atoms C8 (site occupancy factors for C8a/C8b = 0.657(8)/0.343(8)) and C14 (site occupancy factors for C14a/C14b = 0.494(8)/0.506(8)). In the crystal, a disordered water molecule of crystallization (O2W) per molecule of complex was located and refined with an occupancy factor of 0.25. Further crystallographic data and refinement details are summarized in Table 1. Molecular drawings were generated with the ORTEP-3 for Windows application[27] and PLATON.[28] The CCDC reference no. 641477 contains the supplementary crystallographic data of the structure.

Potentiometric Titrations. Acid−base titrations in aqueous 0.1 M KNO_3 solutions were realized using combined glass electrodes connected either to a Potentiograph E536 or a Dosimat 655 (Metrohm) piston buret. Potentiometric measurements coupled with a spectrophotometric detection were carried out in a 50/50 v/v methanol/water mixture containing 0.1 M $NaClO_4·H_2O$ (Merck) in order to keep the ionic strength constant. Standardized 0.1 M acid and base solutions were prepared in the same solvent mixture by dilution of commercial analytical grade $HClO_4$ (Fischer, 70%) and a NaOH concentrate ampule (Merck, Titrisol), respectively. The double-jacketed cell was connected to a Lauda RE106 water circulator ensuring a constant temperature of 298.2(2) K, while the magnetically stirred solutions were maintained under a low-pressure argon stream to exclude CO_2 from the headspace. A PHM240 (Radiometer) ionometer was used to record at 0.1 mV resolution the electromotive force between a high-alkalinity XG200 (Radiometer) glass-bulb electrode and a XR300 (Radiometer) Ag/AgCl reference electrode, which was separated from the bulk of the solution by a sintered-glass bridge filled with 0.1 M $NaClO_4$. To avoid precipitation of $KClO_4$ at the liquid junction, the reference compartment was filled with a saturated NaCl solution containing AgCl. The glass electrode was calibrated prior to each experiment to read hydronium ion concentrations (−log [H_3O^+]), by titrating $HClO_4$ diluted in the supporting electrolyte solution with NaOH. Calibration data were processed according to the four-parameter extended Nernst equation, which takes into account liquid junction potentials.[29] The ionic product of water (pK_w = 13.88(1)) was determined according to the method of Fischer and Byé[30] and fixed in all refinements.

Visible absorption spectra were recorded in situ as a function of −log [H_3O^+] with a Cary 50 Probe (Varian) spectrophotometer equipped with an immersion probe of 1 cm path length made of SUPRASIL 300 (Hellma, reference 661.202). Aliquots of base were added manually with the help of a Gilmont micropipet (2 μL resolution) to a solution containing ∼0.05 mmol of complex. Enough time was allowed after the addition of each base increment in order to reach the equilibrium. The potential-drift criterion was set at dE/dt < 0.1 mV min^{-1}. The collection of absorption spectra was repeated with 2 min delays between two consecutive measurements until identical spectra were obtained. The fitting procedure of the experimental data with the Hyperquad 2006 program[31] has been fully described elsewhere.[29]

Ligand Exchange on an Optically Active Chromium(II) Intermediate. In a 1.00 cm stoppered optical cell containing a pH 7.5 buffered solution (2.5 g, I = 0.1 M), Λ-[Cr^{III}((*S*,*S*)-promp)H$_2$O]ClO$_4$ (3.5 mg, 0.007 mmol), H$_2$(*R*,*R*)-promp·2HCl (0.035 mmol, 5 equiv vs Cr^{III}) and amalgamated zinc (4.6 mg,

Table 1. X-ray Crystallographic Data for Λ-[Cr^{III}((*S*,*S*)-promp)H$_2$O]ClO$_4$·0.25H$_2$O

	Λ-[Cr^{III}((*S*,*S*)-promp)H$_2$O]ClO$_4$·0.25H$_2$O
empirical formula	$C_{17}H_{23.5}ClCrN_3O_{9.25}$
formula weight	505.34
crystal system	monoclinic
space group	$P2_1$
a, Å	11.973(1)
b, Å	7.3331(5)
c, Å	11.979(1)
β, deg	106.08(1)
V, Å^3	1010.5(2)
Z	2
T, K	223(2)
ρ_{calcd}, g cm^{-3}	1.661
μ (Mo Kα), mm^{-1}	0.758
R indices [$I > 2\sigma(I)$][a]	R_1 = 0.0251; wR_2 = 0.0658
R indices (all data)[a]	R_1 = 0.0260; wR_2 = 0.0662

[a] $R_1 = \Sigma||F_o| - |F_c||/\Sigma|F_o|$, $wR_2 = \{\Sigma[w(F_o^2 - F_c^2)^2]/\Sigma[w(F_o^2)^2]\}^{1/2}$.

(26) Sheldrick, G. M. *Acta Crystallogr., Sect. A* **2008**, *64*, 112–122.
(27) Farrugia, L. J. *J. Appl. Crystallogr.* **1997**, *30*, 565.
(28) Spek, A. L. *Acta Crystallogr., Sect. D* **2009**, *65*, 148–155.
(29) Meyer, M.; Frémond, L.; Tabard, A.; Espinosa, E.; Vollmer, G. Y.; Guilard, R.; Dory, Y. *New J. Chem.* **2005**, *29*, 99–108.
(30) Fischer, R.; Byé, J. *Bull. Soc. Chim. Fr.* **1964**, 2920–2929.
(31) Gans, P.; Sabatini, A.; Vacca, A. *Talanta* **1996**, *43*, 1739–1753.

70 mmol, 10 equiv vs Cr^{III}) were introduced. CD spectra between 300 and 600 nm were recorded at a scan rate of 100 nm min^{-1} before and at regular intervals after the zinc addition. The evolution of the total chromium(III) complex concentration was followed by absorbance measurements in the same spectral range. The baseline was recorded with $I = 0.1$ M buffer. The sample was vigorously shaken before each spectroscopic measurement.

Chromium(III) Catalyzed Reduction of Cytochrome *c* by Metallic Zinc. All samples were degassed by gently bubbling argon for at least 15 min and handled in an inert atmosphere. Small volumes were measured with micropipets or weighed. Amalgamated zinc (4.8 mg, 7.30 mmol, 500 equiv vs cyt *c*) and an aqueous H_2(*S*,*S*)-promp·2HCl solution (0.5 mL, 7.30×10^{-3} M, 100 equiv vs cyt *c*, neutralized by some drops of NaOH 0.5 M) were introduced into one compartment of a 2×0.475 cm tandem cell. A freshly prepared solution (0.5 mL) containing cytochrome *c* (7.30×10^{-5} M), Λ-[Cr^{III}((*S*,*S*)-promp)H_2O]ClO_4 (1.46×10^{-3} M, 20 equiv vs cyt *c*) and Tris/HCl buffer (pH 7.5 or 9.0, $I = 0.2$ M) was introduced into the second compartment before thermostatting the cell at the desired temperature. Absorption spectra between 500 and 570 nm were recorded at a scan rate of 100 nm min^{-1} against the buffer solution ($I = 0.2$ M) before and at regular intervals after mixing. The sample was vigorously shaken before each absorbance measurement.

Electrochemical Reduction of Cytochrome *c*. Mercury (38 g), used as the working electrode, was introduced into the electrolytic cell (Metrohm titration vessel with an integrated platinum wire in the bottom). The latter was equipped with an Ag/AgCl reference electrode and the auxiliary electrode (Ag coil fixed on a Metrohm 6.1241.020 support immersed inside a Metrohm 6.1245.000 electrolyte tube containing a 3 M KCl solution and separated from the electrolyzed solution by a ground joint diaphragm). Buffer solution (25 mL, pH 7.5, $I = 0.1$ M) was introduced into the cell and degassed during 5 min by a stream of nitrogen before adding 5 mL of a solution of known concentration containing either cytochrome *c* alone or mixed with the chromium(III) complex. During the whole electrolytic process, the solution was kept under nitrogen and vigorously stirred (2000 rpm) using a magnetic stirrer, while the temperature was maintained constant at 293.0(5) K. The reduction was conducted by applying a fixed potential of −1.5 V between the working and the Ag/AgCl reference electrode (−1.31 V/SHE). The electrolytic current was measured between the working and the auxiliary electrode. The reaction was monitored ex situ by UV−vis absorption spectrophotometry.

Results

Characterization of the Chromium(III) Complexes. Three chromium(III) cationic complexes have been isolated and characterized in the present work, namely, Λ-[Cr^{III}-((*S*,*S*)-promp)H_2O]$^+$, Δ-[Cr^{III}((*R*,*R*)-alamp)H_2O]$^+$, and Λ-[Cr^{III}((*S*,*S*)-alamp)$(H_2O)_2$]$^+$. Rodlike purple crystals of Λ-[Cr^{III}((*S*,*S*)-promp)H_2O]ClO_4·0.25H_2O were grown from an aqueous solution by slow evaporation at room temperature and subjected to X-ray diffraction analysis, whereas plates could also be obtained depending on the perchloric acid concentration of the solution. Crystallographic parameters, data collection, and refinement information are summarized in Table 1. In the crystal, symmetry related molecules are linked via O−H···O hydrogen bonds, involving the coordinated water molecule (O1W) and the carbonyl oxygen atoms (O2 and O4), to form supramolecular helical polymers running parallel to the *b* axis (Figure S1 in the Supporting Information). A disordered water molecule (O2W) was located in a 1:4 ratio with respect to the ion pairs.

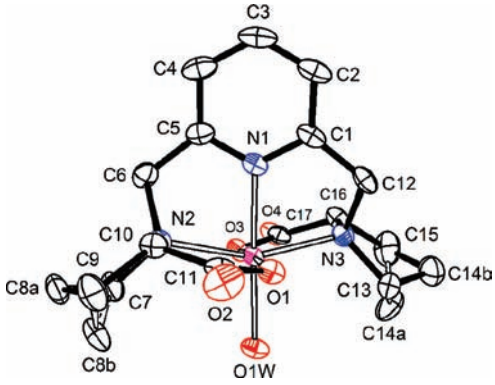

Figure 2. ORTEP view of the Λ-[Cr^{III}((*S*,*S*)-promp)H_2O]$^+$ cation found in the crystal structure of Λ-[Cr^{III}((*S*,*S*)-promp)-H_2O]ClO_4·0.25H_2O showing the atom-labeling scheme and the thermal ellipsoids at the 50% probability level. The carbon atoms C8a/C8b and C14a/C14b belonging to the proline rings are disordered. The minor conformer corresponding to C8b and C14a is represented by dashed bonds. Hydrogen atoms have been omitted for clarity.

An ORTEP view of the crystal structure of [Λ-[Cr^{III}((*S*,*S*)-promp)H_2O]$^+$ is shown in Figure 2 together with the atom labels. Both aminocarboxylate rings of the (*S*,*S*) enantiomer afford a Λ configuration of the donor atoms around the metal center. As already observed for the corresponding cobalt(III) complex,[32] both five-membered pyrrolidine cycles adopt an envelope-type conformation in which the most out-of-plane carbon atom is disordered over two positions, noted a and b, with refined site occupation factors of 0.657(8)/0.343(8) and 0.491(8)/0.509(8) for C8a/C8b and C14a/C14b, respectively. The chromium(III) center is embedded in a distorted octahedron with an O_2N_2 basal plane (N2, O1, N3, and O3), while the pyridyl nitrogen atom (Cr−N1 = 1.986(2) Å) and one bound water molecule (Cr−O1W = 2.006(2) Å) occupy the axial positions. Other typical bond lengths and bond angles are summarized in Table 2 together with the corresponding values found for the analogous cobalt(III) compound.[32] All the M−O bond length differences between the chromium and cobalt complexes reported in Table 2 correspond almost to the ionic radii change of both metals. Conversely, the differences in the M−N distances, especially those pertaining to the M−N1 and M−N3 bonds that reach 12%, are significantly larger and thus reflect the lower affinity of Cr^{3+} for a nitrogen donor atom. It appears that the coordination polyhedron is more distorted for chromium than cobalt. The largest deviation from an ideal octahedron occurs in the Cr−N2 bond (Cr−N2 = 2.097(2) Å), while the smallest angle (N1−Cr−N3) reaches 78.7(1)° instead of 90°. As a general trend, the N1−M−N angles are considerably smaller than 90° in comparison with the N1−M−O angles which are more regular for both chromium and cobalt complexes, because the five-membered chelate rings containing these atoms are rigid due to the aromatic C−N1 bonds and cannot compensate the strain imposed by the metallic center. On the basis of these remarks, it might therefore be anticipated that the overall stability of the chromium(III) complex would be lower compared to the cobalt(III) analogue.

(32) Sauvain, J. J. Ph.D. Thesis, Université de Neuchâtel: Neuchâtel, Switzerland, 1990.

Table 2. Comparison of Selected Bond Lengths (Å) and Angles (deg) Involving the Coordination Center for Λ-[M^{III}((*S*,*S*)-promp)H_2O]ClO_4[a]

	M = Cr	M = Co[b]		M = Cr	M = Co[b]
M−O1	1.929(2)	1.871(3)	M−N1	1.986(2)	1.846(3)
M−O3	1.946(2)	1.885(3)	M−N2	2.097(2)	1.871(3)
M−O1W	2.006(2)	1.961(3)	M−N3	2.095(2)	1.871(3)
N1−M−N2	79.3(1)	82.2(1)	N2−M−O3	96.5(1)	93.6(1)
N1−M−N3	78.7(1)	82.6(1)	N3−M−O1	96.8(1)	92.5(1)
N1−M−O1	90.0(1)	90.4(1)	N3−M−O1W	100.2(1)	96.1(1)
N1−M−O1W	177.2(1)	177.6(1)	N3−M−O3	83.6(1)	87.2(1)
N1−M−O3	94.6(1)	94.3(1)	O1−M−O1W	87.5(1)	87.7(1)
N2−M−N3	157.9(1)	164.8(1)	O1−M−O3	175.4(1)	175.2(1)
N2−M−O1	84.8(1)	87.9(1)	O3−M−O1W	87.9(1)	87.6(1)
N2−M−O1W	101.8(1)	99.1(1)			

[a] Uncertainties on the last digits are indicated in parentheses. The atom numbering scheme is shown in Figure 2. W = coordinated water molecule. [b] M = Co, data taken from ref 32.

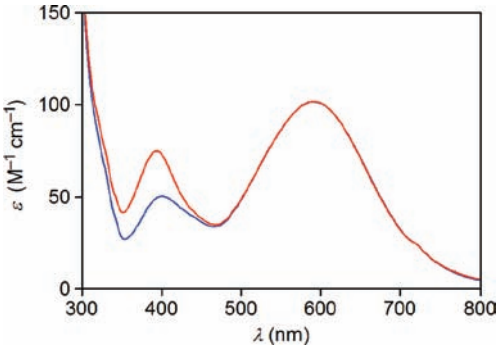

Figure 3. Molar absorptivities of Δ-[Cr^{III}((*R*,*R*)-alamp)H_2O]ClO_4, c = 1.6×10^{-3} M (blue line) and Λ-[Cr^{III}((*S*,*S*)-alamp)$(H_2O)_2$]ClO_4, c = 1.9×10^{-3} M (red line). Spectra were recorded at pH 4.0.

Unfortunately, the Λ and Δ enantiomers of the complexes incorporating the $alamp^{2-}$ ligand did not crystallize. In the absence of X-ray crystal data, their structure was probed by absorption and CD spectroscopy. In the 450−700 nm wavelength range, the absorption spectra of [Cr^{III}((*S*,*S*)-alamp)$(H_2O)_2$]$^+$ and [Cr^{III}((*R*,*R*)-alamp)-H_2O]$^+$ are superimposable, as expected for a similar set and arrangement of donor atoms coordinated on the metal center (Figure 3). However, at wavelengths below 450 nm, significant differences appear in the absorption spectra. This might be indicative of a different binding scheme of the ligand around the metal ion, one of the carboxylate groups in [Cr^{III}((*S*,*S*)-alamp)$(H_2O)_2$]$^+$ being replaced by a second water molecule.

Between 350 and 650 nm, [Cr^{III}((*S*,*S*)-alamp)$(H_2O)_2$]$^+$ exhibits almost the same CD pattern than Λ-[Cr^{III}((*S*,*S*)-promp)H_2O]$^+$ (Figure 4). This confirms the supposed Λ configuration of its metal center. As the CD spectrum of [Cr^{III}((*R*,*R*)-alamp)H_2O]$^+$ is nearly symmetrical to the one of Λ-[Cr^{III}((*S*,*S*)-alamp)$(H_2O)_2$]$^+$, a Δ configuration is assigned to the chromium complex with the (*R*,*R*)-$alamp^{2-}$ ligand. Furthermore, the similar spectroscopic properties exhibited by the Cr^{3+} compounds and their Co^{3+} analogues confirm their unique structure with predetermined chirality.[3]

The acid−base behavior of both Δ-[Cr^{III}((*R*,*R*)-alamp)H_2O]$^+$ and Λ-[Cr^{III}((*S*,*S*)-alamp)$(H_2O)_2$]$^+$ complexes has been investigated by means of absorption spectrophotometry in a binary methanol/water 50/50 v/v

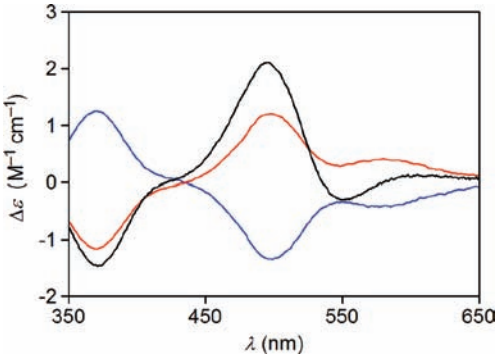

Figure 4. Molar dichroic absorption coefficients of Δ-[Cr^{III}((*R*,*R*)-alamp)H_2O]ClO_4, c = 1.6×10^{-3} M (blue line); Λ-[Cr^{III}((*S*,*S*)-alamp)-$(H_2O)_2$]ClO_4, c = 1.9×10^{-3} M (red line); and Λ-[Cr^{III}((*S*,*S*)-promp)H_2O]ClO_4, c = 1.0×10^{-3} M (black line). Spectra were recorded at pH 4.0.

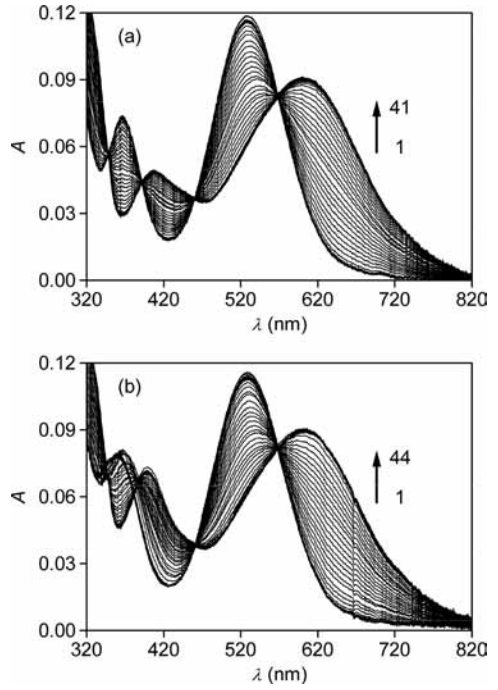

Figure 5. Spectrophotometric titrations by 0.1 M NaOH of Δ-[Cr^{III}((*R*,*R*)-alamp)H_2O]ClO_4, c_0 = 9.2×10^{-4} M, V_0 = 50 mL, spectra 1−41: −log [H_3O^+] = 2.41−10.54 (panel a) and Λ-[Cr^{III}((*S*,*S*)-alamp)-$(H_2O)_2$]ClO_4, c_0 = 1.00×10^{-3} M, V_0 = 50 mL, spectra 1−44: −log [H_3O^+] = 2.32−11.14 (panel b). Solvent: MeOH/H_2O 50/50 v/v, I = 0.1 M ($NaClO_4$), T = 298.2(2) K, l = 1 cm.

solvent mixture at constant ionic strength (I = 0.1 M $NaClO_4$) and temperature (T = 298.2(2) K). For each compound, a typical set of spectra recorded as a function of −log [H_3O^+] is shown in Figure 5. Principal component analysis of the entire data matrix collected for Δ-[Cr^{III}((*R*,*R*)-alamp)H_2O]$^+$ (Figure 5a) clearly supports a model with a single equilibrium. Subsequent nonlinear least-squares analysis of three independent experiments provided an average pK_a value of 6.54(2) for the deprotonation of the metal-bound water molecule. The calculated electronic spectrum of Δ-[Cr^{III}((*R*,*R*)-alamp)H_2O]$^+$ (λ_{max} = 366 nm, ε = 81 M^{-1} cm^{-1}; λ_{max} = 528 nm, ε = 130 M^{-1} cm^{-1}) undergoes both bathochromic and hypochromic shifts upon formation of the hydoxo species (λ_{max} = 407 nm, ε = 56 M^{-1} cm^{-1}; λ_{max} = 600 nm, ε = 102 M^{-1} cm^{-1}).

Table 3. Cathodic (E_{pc}) and Anodic (E_{pa}) Peak Potentials, Half-Wave Potentials ($E_{1/2}$), and Peak-to-Peak Separation (ΔE) of Λ-[M((*S*,*S*)-promp)H_2O]ClO_4 and Δ-[M((*R*,*R*)-(alamp)H_2O]ClO_4 Expressed in Volts vs SHE[a]

	Λ-[M((*S*,*S*)-promp)H_2O]$^+$				Δ-[M((*R*,*R*)-(alamp)H_2O]$^+$			
M	E_{pc}	E_{pa}	$E_{1/2}$	ΔE	E_{pc}	E_{pa}	$E_{1/2}$	ΔE
Cr	−1.05[b]	−0.97[b]	−1.01[b]	0.08[b]	−1.09[b]	−1.01[b]	−1.05[b]	0.08[b]
Fe	+0.12[c]				+0.02[c]			
Co	−0.14[c]				−0.20[c]			

[a] Scan rate: 50 mV s^{-1}. Half-wave potentials for quasi-reversible systems correspond to the average of E_{pc} and E_{pa}. [b] pH = 7.5 (Tris/HCl), I = 0.1 M. [c] pH = 4.5 (CH_3CO_2H/$NaCH_3CO_2$), I = 0.1 M, data taken from ref 33.

In contrast, the spectral changes recorded below 450 nm upon base addition to a solution of Λ-[Cr^{III}((*S*,*S*)-alamp)$(H_2O)_2$]$^+$ (Figure 5b) is compatible with the presence of a third absorbing species between pH 5 and 8. However, the potentiometric titration curves show only a single buffer region in that pH range with a first equivalence point corresponding to the neutralization of the strong acid in excess and a second one to the addition of an apparent equimolar amount of base. While this result is in apparent contradiction with the spectrophotometric data recorded in the same pH range, it might be rationalized by assuming that the complex is present in solution as a dimer under acidic conditions. This assumption was further corroborated by ESI-MS, which highlights the propensity of the Λ-isomer to form most probably methoxy-bridged dimers in a methanol rich solvent. Although elemental analysis and high-resolution ESI-MS data provided strong evidence for a pure substance, no satisfactory fit could be obtained for that compound.

Electrochemical Studies of the Chromium(III) Complexes. The electrochemical behavior of the three prepared complexes was investigated by cyclic voltammetry (CV) at a hanging mercury drop electrode in an aqueous Tris/HCl buffer at pH 7.5 (I = 0.1 M). Given the pK_a values of about 7 measured for Λ-[Cr^{III}((*S*,*S*)-promp)H_2O]$^+$ and Δ-[Cr^{III}((*R*,*R*)-alamp)H_2O]$^+$, the recorded traces correspond in fact to mixtures with the neutral Λ-[Cr^{III}((*S*,*S*)-promp)OH] and Δ-[Cr^{III}((*R*,*R*)-alamp)OH] species, respectively. For both substances, the voltammograms recorded at a scan rate of v = 50 mV s^{-1} evidenced a quasi-reversible single wave centered at −1.01 and −1.05 V/SHE (Figure S2 in the Supporting Information), respectively, that can be attributed to a one-electron transfer from the Cr(III) to the Cr(II) complexes. The peak and half-wave potentials are summarized in Table 3, together with the electrochemical parameters corresponding to the cobalt and iron analogues for sake of comparison.[33] The peak separation (ΔE = 80 mV) is slightly larger than the theoretical 58 mV for a fast single electron transfer and increased with faster scan rates to reach 100 mV at v = 300 mV s^{-1} (Figure S2 in the Supporting Information). The quasi-reversibility was also pointed out by systematically higher reduction versus oxidation peak currents, although the $|i_{pc}|/|i_{pa}|$ ratio remained approximately constant at ∼1.1 over the 25−300 mV s^{-1} scan-rate range. The intensities were found to vary linearly with respect to $v^{1/2}$. The quasi-reversible behavior of the investigated [Cr^{III}(L)]$^+$/[Cr^{II}(L)] redox systems suggests that the mean lifetime of the Cr^{II} species generated at the surface of the electrode corresponds at least to the scan time (∼10 s).

In addition to the reduction and oxidation peaks located at −1.05 and −0.97 V/SHE, respectively, the CV curves pertaining to Λ-[Cr^{III}((*S*,*S*)-promp)H_2O]$^+$ show two unexpected sharp peaks at −0.96 and −0.94 V/SHE which were slightly shifted, respectively, to more negative (cathodic) and more positive (anodic) values when the scanning rate was increased (Figure S2 in the Supporting Information). These waves are most likely due to the adsorption, respectively, desorption, of the positively charged complex on the surface of the mercury drop. The fact that such peaks did not appear for both alamp^{2-} complexes could be understood in terms of structural and lipophilicity differences between promp^{2-} and alamp^{2-}.

Whereas the electrochemical properties of Δ-[Cr^{III}((*R*,*R*)-alamp)H_2O]$^+$ are very similar to those of Λ-[Cr^{III}((*S*,*S*)-promp)H_2O]$^+$, with slightly more negative peak potentials (Figure 10), striking differences are observed for Λ-[Cr^{III}((*S*,*S*)-alamp)$(H_2O)_2$]$^+$. As shown in Figure 6, a strong cathodic wave with a shoulder at −1.16 V/SHE and a peak at −1.3 V/SHE are observed, the latter vanishing at higher scan rates (Figure S2 in the Supporting Information). However, the anodic wave and the associated peak potential are similar for both alamp^{2-} complexes, suggesting that the quasi-reversible [Cr^{III}(L)]$^+$/[Cr^{II}(L)] redox system overlaps with irreversible processes occurring at more negative potentials. As the intensity of this wave is about 10 times higher than the reduction current of the Cr^{III} complex and as there is no corresponding anodic part, this feature suggests an electrocatalytic reduction of water. To confirm this assumption, bulk electrolysis on a large area mercury pool of a 10^{-3} M solution was conducted under similar conditions by applying a constant working potential of −1.16 V/SHE. The electrocatalytic process was monitored until the current dropped to zero for an overall Coulombic charge greatly exceeding the value expected for a one-electron reduction of the chromium(III) complex. Indeed, integration of the current during the electrolysis leads to an overall charge corresponding to nearly nine equivalents of electrons versus the molar quantity of the complex. Moreover, gas evolution was evidenced visually by the observation of bubbles, while molecular hydrogen formation was formally identified by the $PdCl_2$ assay.[24,25] In contrast, no catalytic current nor hydrogen formation could be detected in the control experiments conducted at the same potential on a pure buffer solution and in the presence of Δ-[Cr^{III}((*R*,*R*)-alamp)H_2O]$^+$ (one equivalent of electron was consumed per mole of complex in that case).

Tentative Isolation of Chromium(II) Complexes. The preparation of solutions containing [Cr^{II}((*S*,*S*)-promp)] for further use as chiral reducing agent was attempted by reacting $CrCl_2$ solutions with the considered ligand under anaerobic conditions. As the direct metalation reaction turned out to be unsuccessful, the favorable electrochemical properties outlined above prompted us to consider next the possibility to reduce quantitatively Λ-[Cr^{III}((*S*,*S*)-promp)H_2O]$^+$ either by chemical means with metallic

(33) Hilgers, H. J.; Bernauer, K. *Inorg. Chim. Acta* **1998**, *275*−*276*, 9–14.

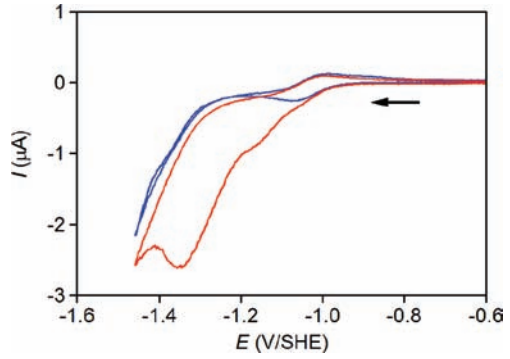

Figure 6. Cyclic voltammograms on a hanging mercury drop electrode of Δ-[Cr^{III}((*R*,*R*)-alamp)H_2O]ClO_4 (blue line) and Λ-[Cr^{III}((*S*,*S*)-alamp)-$(H_2O)_2$]ClO_4 (red line). [complex] = 4×10^{-4} M, pH = 7.5 (Tris/HCl), I = 0.1 M, scan rate: 100 mV s^{-1}.

Zn or electrochemically by applying a fixed potential on a pool of mercury ($E = -1.31$ V/SHE). However, all these attempts failed also, as no chromium(II) complex could be isolated or even identified in the reaction mixture by visible absorption spectrophotometry. The Cr^{2+} complex is therefore produced only as a transient species that is rapidly reoxidized by water due to the highly negative electrochemical potential. We therefore checked whether or not the lifetime of the reduced state would be sufficiently long in order to be used in situ.

Reduction-Induced Transchelation Experiments. An easy way for testing the aforementioned hypothesis was to investigate the kinetics of the self-exchange reaction with the corresponding enantiomeric ligand by chiroptical methods. When an excess of H_2(*R*,*R*)-promp was added to a solution of Λ-[Cr^{III}((*S*,*S*)-promp)H_2O]$^+$, no reaction was observed even at elevated temperature or after a long period of time. On the other hand, when amalgamated Zn was present in the mixture, the CD spectrum smoothly changed to that of its enantiomer (Figure 7), although the opposite ellipticity values could not be reached for the final spectrum pointing toward an equilibrium situation. The 5-fold excess of H_2(*R*,*R*)-promp plays a double role: on the one hand it binds the formed Zn^{2+} in order to shift the reduction potential of zinc to sufficiently negative values and, on the other hand, it allows the formation of an excess of the enantiomeric Cr^{III} complex. As shown in Figure 7, the reaction proceeds after a short induction period until an equilibrium situation is reached that corresponds to the concentration ratio of the two enantiomeric ligands. As the chromium(III) compound is inert, the ligand self-exchange necessarily involves the transient formation of the corresponding chromium(II) species, the latter being rapidly reoxidized either by the chromium(III) compounds present or by water according to Figure 8. Control measurements showed that the UV−vis spectrum of the reaction mixture remained almost unchanged, indicating that the concentration of the Cr^{II} species is kept at a low level during the whole duration of the reaction.

Chromium(III) Catalyzed Reduction of Cytochrome *c* by Metallic Zinc. On the basis of the results outlined thus far, the electron-transfer reaction between cytochrome *c* and the in situ produced labile chromium(II) complexes could be reasonably envisioned. It was first ascertained that no reaction occurred by simply mixing the trivalent chromium complexes with a native or chemically reduced protein solution. This result was in agreement with those obtained previously for the corresponding cobalt(III) complexes and were expected because of the high inertia of the trivalent chromium and cobalt species.[11] If the aforementioned electron-transfer mediated ligand self-exchange reaction supports the existence of a short-lived labile chromium(II) species in solution, it does not yet guarantee that the low-valent metal complexes are able to act as a reducing agent of metalloproteins, in spite of their much lower redox potential compared to the value reported for cytochrome *c* (+0.26 V/SHE at pH 7 and 25 °C).

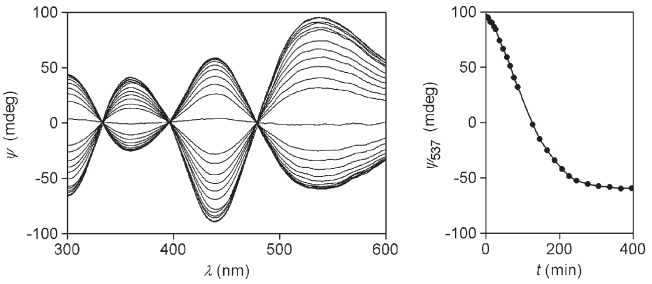

Figure 7. Evolution of the CD signal during the ligand self-exchange reaction of Λ-[Cr^{III}((*S*,*S*)-promp)H_2O]ClO_4 ($c_0 = 2.81 \times 10^{-3}$ M) with H_2(*R*,*R*)-promp ($c_0 = 1.44 \times 10^{-2}$ M) in the presence of 7.8 equiv of Zn/Hg. The time course of the reaction monitored at 537 nm is shown on the right side (the line was drawn as an eye guide only). T = 302.4(2) K, pH = 7.7, l = 1 cm.

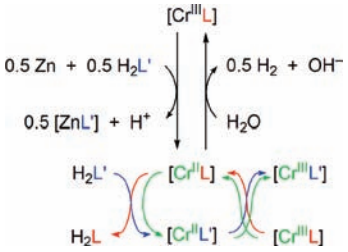

Figure 8. Electron transfer mediated ligand self-exchange reaction on Λ-[Cr^{III}(promp)H_2O]ClO_4. L = (*S*,*S*)-$promp^{2-}$; L′ = (*R*,*R*)-$promp^{2-}$. Charges and coordinated water molecules have been omitted for clarity.

For thermodynamic reasons, cytochrome *c* complex should be reduced first by metallic zinc. As a matter of fact, a kinetic control of the system is required, allowing the reduction of the Cr^{III} complex and the consecutive reoxidation of the formed Cr^{II} species by cytochrome *c* to be much faster than the direct reduction of the latter. In that way the [Cr^{III}(L)]$^+$/[Cr^{II}(L)] system should function as an electron-transfer catalyst. Indeed, spectrophotometric monitoring of a mixture containing a 20-fold excess of Λ-[Cr^{III}((*S*,*S*)-promp)H_2O]$^+$ with respect to cytochrome *c*, free ligand, and amalgamated zinc revealed the expected spectral modifications of the B (also denoted as Soret) and Q bands of the heme moiety as the redox state of the iron center changes from +III (λ_{max} = 412, 530 nm) to +II (λ_{max} = 418, 518, 548 nm).[34] It is therefore concluded that most of the protein is reduced by the in situ generated [Cr^{II}((*S*,*S*)-promp)] complex. The kinetic traces recorded in the Q-band region at the most intense

(34) Harbury, H. A.; Marks, R. H. L. In *Inorganic Biochemistry*; Eichhorn, G. L., Ed.; Elsevier: London, 1973; Vol. *2*, pp 902−954.

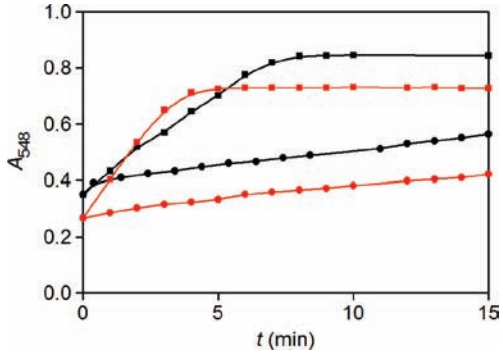

Figure 9. Reduction kinetics of horse-heart cytochrome *c* by amalgamated zinc in the absence (dots) or in the presence of 20 equiv of Λ-[Cr^{III}((S,S)-promp)H_2O]ClO_4 (squares) at pH 7.6 (black curves) and pH 9.0 (red curves) monitored by absorption spectrophotometry at 548 nm. The lines were drawn as an eye guide only. $[cyt\ c]_0 = 3.65 \times 10^{-5}$ M, $[H_2(S,S)\text{-promp}] = 3.8 \times 10^{-3}$ M, 2000 equiv Zn/Hg, $I = 0.1$ M (Tris/HCl buffer), $T = 327.3(2)$ K, $l = 1$ cm.

absorption maxima of the ferrous state (548 nm) are reproduced in Figure 9. They show that the reduction rate of cytochrome *c* by amalgamated zinc is enhanced by a factor of about 10 in the presence of the chiral chromium complex. At pH 9.0, this catalytic effect is about twice as high compared to that observed at pH 7.5.

Electrolytic Reduction of Cytochrome *c* Catalyzed by Chromium(III) Complexes. Reduction of cytochrome *c* by the Cr^{II} complex produced in situ by amalgamated zinc is a heterogeneous process, which precludes an exact control of the reaction conditions. In turn, such a control can easily be achieved by electrochemistry. We therefore examined hereafter the electrochemical behavior of the three complexes in the presence of cytochrome *c*, as well as that of the pure protein. The corresponding CVs are presented in Figure 10. The curve corresponding to cytochrome *c* alone in the Tris/HCl buffer at physiological pH highlights the absence of electrochemical activity down to −1.15 V/SHE. The growing cathodic current recorded down to −1.30 V/SHE indicates however the possibility to reduce the protein at more negative potentials.

When cytochrome *c* was added to a solution containing 10 equiv of either complex, the cyclic voltammograms remained almost unchanged at a given scan rate of 50 or 100 mV s^{-1} (Figure 10). Interestingly, the adsorption peaks overlapping with the cathodic and anodic signals found for Λ-[Cr^{III}((*S*,*S*)-promp)H_2O]$^+$ completely disappeared in the presence of cytochrome *c*. It is known that the positively charged protein is strongly adsorbed at the mercury surface and might prevent the adsorption of the complex by reducing the charge density on the surface of the electrode.[35,36] The slight deviations occurring at potentials beyond the cathodic peak are due to the reduction of the protein. This was ascertained by comparing the experimental curves with those obtained by summing the CV responses corresponding to the pure complex and the protein alone. The almost perfect match reveals that the direct electrocatalytic reduction of cyto-

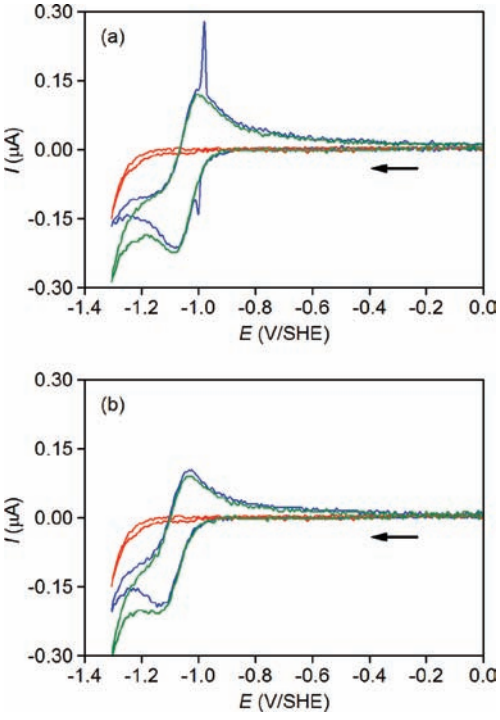

Figure 10. Cyclic voltammograms on a hanging mercury drop electrode of cytochrome *c* (red line) and of the chromium(III) complexes either alone (blue line) or in the presence of the protein (green line); panel a, Λ-[Cr^{III}((*S*,*S*)-promp)H_2O]ClO_4; panel b, Δ-[Cr^{III}((*R*,*R*)-alamp)H_2O]-ClO_4. [cyt *c*] = 4×10^{-5} M, [complex] = 4×10^{-4} M, pH = 7.5 (Tris/HCl), $I = 0.1$ M, scan rate: 50 mV s^{-1}.

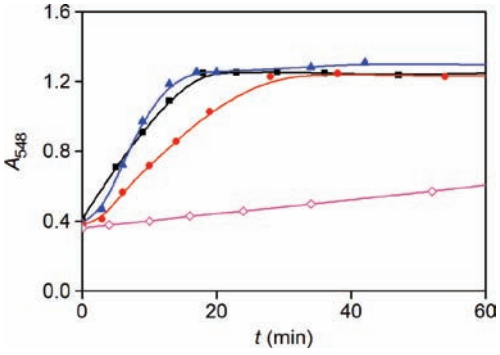

Figure 11. Time-evolution of the absorbance measured at 548 nm during the electrochemical reduction at −1.5 V vs Ag/AgCl (−1.31 V/SHE) on a mercury layer electrode of horse-heart ferricytochrome *c* alone (pink ◇) or in the presence of either Λ-[Cr^{III}((*S*,*S*)-promp)H_2O]ClO_4 (black ■), Δ-[Cr^{III}((*R*,*R*)-alamp)H_2O]ClO_4 (blue ▲), or Λ-[Cr^{III}((*S*,*S*)-alamp)$(H_2O)_2$]ClO_4 (red ●). The lines were drawn as an eye guide only. [cyt *c*] = 4×10^{-5} M, [complex] = 4×10^{-4} M, pH = 7.5 (Tris/HCl), I = 0.1 M, $T = 293.0(5)$ K, $l = 1$ cm.

chrome *c* is negligible during the sweep time, as any catalytic effect (EC mechanism) should have given rise to a cathodic peak current enhancement together with a lowering of the anodic peak current intensity. Considering the reversibility of the [Cr^{III}(L)]$^+$/[Cr^{II}(L)] system on the second time scale (i.e., the sweep time) and the absence of any characteristic feature for electrocatalysis in the cyclic voltammograms, it can therefore be safely concluded that the intermolecular electron transfer and/or concomitant reduction of the heme unit of cytochrome *c* should take much longer. This observation is in qualitative agreement with the kinetic measurements performed

(35) Sevilla, J. M.; Pineda, T.; Roman, A. J.; Manuedo, R.; Blazquez, M. *J. Electroanal. Chem.* **1998**, *451*, 89–93.
(36) Buleandra, M.; Radu, G. L.; Tanase, I. *Roum. Biotechnol. Lett.* **2000**, *5*, 423–438.

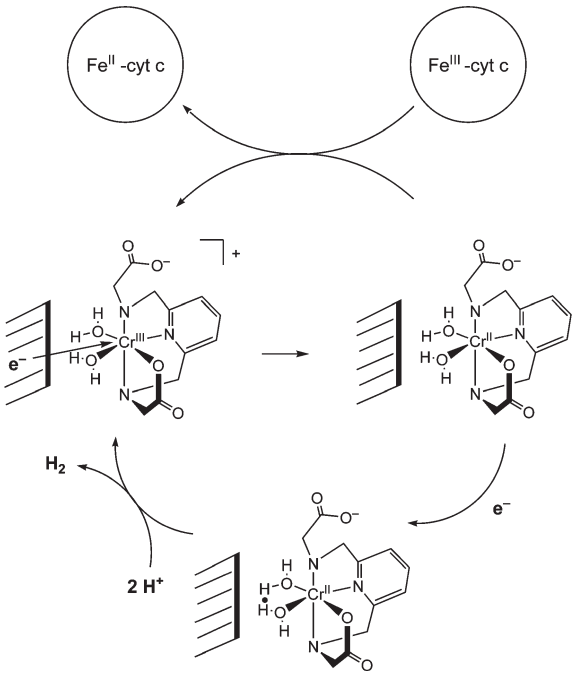

Figure 12. Proposed mechanism for the concurrent reduction of cytochrome *c* and water by Λ-[Cr^{III}((*S*,*S*)-alamp)(H$_2$O)$_2$]ClO$_4$.

under heterogeneous conditions using amalgamated zinc powder as the chemical reducing agent.

In order to corroborate this hypothesis, chiral Cr^{II} complexes were therefore generated in situ in the presence of the protein by electrolysis at constant potential (−1.31 V/SHE) on a large mercury layer electrode. The time evolution of the spectroelectrochemical data collected in the visible range for all three complexes prepared herein (Figures S3−S5 in the Supporting Information) evidence the reduction of cytochrome *c*; the spectral changes accompanying the reduction of the ferric heme to the ferrous state being identical to those recorded for the chemically induced reaction using metallic zinc. A typical set of kinetic traces recorded at 548 nm, both in the absence and presence of chromium complexes, is shown in Figure 11. These results confirm those obtained by cyclic voltammetry. The uncatalyzed electrochemical reduction of cytochrome *c* is very slow. Under the prevailing conditions, about 20% of the protein are reduced after 1 h. Moreover, open-circuit control measurements indicated a slow reduction, accompanied by a slow decomposition over the same period. This chemical degradation is roughly two times slower compared to the electrochemical one. In contrast, the absorbance increases sharply and almost linearly with time as soon as the potential is applied to an electrochemical cell containing both cytochrome *c* and a 10-fold excess of Λ-[Cr^{III}((*S*,*S*)-promp)H$_2$O]$^+$ or Δ-[Cr^{III}((*R*,*R*)-alamp)H$_2$O]$^+$ (Figure 11). A plateau is reached after ∼20 min corresponding to the complete conversion to the ferrous state as evidenced by the typical Q-band pattern with absorption maxima at 518 and 548 nm. As for the zinc promoted reduction, there is no induction period during the initial stage. From the slope of the linear portion, it is inferred that the electrochemical reduction rate increases by a factor of about 20 when the chiral complexes are added, while the catalytic effect of Λ-[Cr^{III}((*S*,*S*)-alamp)(H$_2$O)$_2$]$^+$ is somewhat lower as it takes about 40 min to reach the equilibrium situation. Overall, the reduction of cytochrome *c* is much slower, at least by a factor of about 100, than the oxidation of the Cr^{II} species formed during a cyclic voltammetric experiment performed at a scan rate of 100 mV s^{-1}. This result perfectly agrees with the quasi-reversible shape of the cyclic voltammograms recorded in the presence of protein and chromium(III) complexes, as they correspond to a degenerate EC system with an exceedingly slow chemical step in comparison with the [Cr^{III}(L)]$^+$/[Cr^{II}(L)] electron transfer kinetics.

Discussion

Highly stable and inert chromium(III) complexes have been obtained in a straightforward manner by reacting CrCl$_3$·6H$_2$O or KCr(SO$_4$)$_2$·12H$_2$O with optically pure pentadentate ligands incorporating alanine (alamp^{2-}) or proline (promp^{2-}) amino acid residues. As previously reported for the cobalt(III) analogues,[2] a *R* configuration of both asymmetric carbon atoms of alamp^{2-} or promp^{2-} induces an absolute Δ configuration around the metal center, as evidenced by X-ray crystallography and circular dichroism spectroscopy. Conversely, the *S*,*S* enantiomer promotes exclusively the formation of complexes possessing a Λ chirality, which cannot undergo racemization. Most strikingly, reacting CrCl$_3$·6H$_2$O with both optical isomers of H$_2$alamp under slightly different conditions did not afford the expected pair of enantiomers. Instead, two complexes with the expected opposite chirality but differing by their composition and structural formula (i.e., the number of coordinated water molecules) were isolated. While both compounds displayed their own acid−base and electrochemical properties, it also turned out that conversion of the mono- to the diaquo species or vice versa did not occur in neutral or acidic medium. However, deprotonation of the bound water molecule for the monoaquo complexes Δ-[Cr^{III}-((*R*,*R*)-alamp)H$_2$O]$^+$ and Λ-[Cr^{III}((*S*,*S*)-promp)H$_2$O]$^+$ is characterized with pK_a values slightly lower than 7.

The apparent half-wave potentials listed in Table 3 for Λ-[Cr^{III}((*S*,*S*)-promp)H$_2$O]$^+$ and Δ-[Cr^{III}((*R*,*R*)-alamp)-H$_2$O]$^+$ at pH 7.5 in the Tris/HCl buffer correspond to mixtures of the aquo and hydroxo species. These values are shifted by more than −600 mV with respect to the Cr^{3+}/Cr^{2+} standard redox potential (−0.407 V/SHE). According to the Nernst equation, a 59 mV shift to more negative values of the redox potential for a single electron transfer translates into an increase by 1 order of magnitude of the ratio of the equilibrium constants β([Cr^{III}(L)]$^+$)/β([Cr^{II}(L)]). Hence, the electrochemical data clearly indicate that this ratio reaches at least 10 orders of magnitude for the considered alamp^{2-} and promp^{2-} complexes. Moreover, this stability difference agrees well with that observed for the corresponding iron complexes.[33] By comparison, the Cr$^{III/II}$ redox potential of the macrocyclic complex [Cr^{II}([15]aneN$_4$)(H$_2$O)$_2$]$^{2+}$ is significantly less negative (−0.58 V/SHE at I = 0.4 M HClO$_4$),[37] indicating a much lower stability difference between the bi- and trivalent metal complexes. Accordingly, this macrocyclic compound is much easier to handle than the aminocarboxylate complexes described herein in electron transfer reactions with metalloproteins.[21,37]

Furthermore, the case of Λ-[Cr^{III}((*S*,*S*)-alamp)(H$_2$O)$_2$]$^+$ deserves some additional comments. The cathodic wave,

(37) Samuels, G. J.; Espenson, J. H. *Inorg. Chem.* **1979**, *18*, 2587–2592.

which is not observed for Δ-[Cr^{III}((*R*,*R*)-alamp)H_2O]$^+$, can be attributed to the catalytic reduction of the coordinated water molecules to molecular hydrogen as evidenced by the $PdCl_2$ test.[24,25] The peak potential corresponding to this reaction is more negative than the one assigned to the reduction of the coordination center. The reduced complex can react in two ways as schematically shown in Figure 12: either it reduces the cytochrome *c* present at the surface of the cathode in agreement with the observed catalytic effect or it accepts a second electron leading to the reduction of the coordinated water molecules. As this reaction is not observed for Δ-[Cr^{III}((*R*,*R*)-alamp)H_2O]$^+$ by cyclic voltammetry, it seems that the rapid formation of molecular hydrogen during the scan time needs the presence of two water molecules located in a cis-position in the coordination sphere of the chromium center.

The intended use of chiral chromium complexes was sought as an expedient for probing the stereospecificity and mechanism of the electron-transfer reaction with a test protein, namely, cytochrome *c*. In previous works, optically active iron(II)[9] or cobalt(II)[11,38] complexes formed with $alamp^{2-}$ and $promp^{2-}$ were used as reducing agents. One of the solvent exposed histidine residue (His-26 or the His-33) was shown to act as a bridge in the electron transfer path between [Co^{II}(alamp)] and the iron(III) center embedded in the heme. Dialysis experiments performed at the end of the reaction also revealed that ~43% of the inert Δ-[Co^{III}((*R*,*R*)-alamp)]$^+$ was bound to the protein via the coordination of an imidazole group of the involved histidine fragment, while the amount of fixed Λ enantiomer reached only 15% with respect to the initial quantity. The observed enantioselectivity was assigned to a chiral recognition of the inner-sphere reducing agent by the binding pocket of the protein.

Spurred by these findings, the initial aim of the present study was to explore further the enantioselectivity of the electron transfer reaction mediated by the labile but configurationally stable chromium(II) complexes acting as powerful reducing agents. Unfortunately, the first prerequisite for achieving that goal could not be fulfilled herein, as (*R*,*R*)- and (*S*,*S*)-$alamp^{2-}$ afforded two complexes differing not only by their chirality but also by their nature and structure, probably as a consequence of slightly different preparation methods. Thus, it becomes inherently difficult to assign any difference in their reactivity to only one or to both factors. In agreement with the previous results obtained for Λ-[Co^{III}((*S*,*S*)-promp)H_2O]$^+$,[38] the corresponding chromium analogue appeared less well suited for that purpose most probably because of the steric hindrance imposed by the proline cycles which form a kind of protecting belt around the metal center. Indeed, electron-transfer mediated fixation assays on ferricytochrome *c* using amalgamated zinc failed as no significant difference was observed between the CD spectra of the dialyzed protein recovered after reduction performed both in the presence and in the absence of chromium salt. Thus, no efforts were made to synthesize and test the Δ-[Cr^{III}((*R*,*R*)-promp)H_2O]$^+$ enantiomer.

Absorption spectrophotometric monitoring of the reduction of cytochrome *c* enabled one to demonstrate that the in situ generated chromium(II) complexes strongly accelerate the overall process. The rates of the electrochemical reaction involving Δ-[Cr^{III}((*R*,*R*)-alamp)H_2O]$^+$ and Λ-[Cr^{III}((*S*,*S*)-promp)H_2O]$^+$ are almost identical, while Λ-[Cr^{III}((*S*,*S*)-alamp)$(H_2O)_2$]$^+$ is somewhat less reactive probably as a consequence of the formation of molecular hydrogen as a side reaction. Interestingly, the chemical reduction by metallic zinc and the catalyzed electrochemical reaction proceed with very similar rates, indicating that the rate-determining step is the reaction between the protein and the chromium(II) complex and not the formation of the latter. For chemical and electrochemical processes, zero-order kinetics is observed, suggesting that the reaction proceeds at the surface of either the metallic zinc particles or the mercury electrode, the concentrations of the reacting species on the surface remaining nearly constant during the reaction. For the zinc-mediated reduction, the catalytic effect evidenced by Figure 9 is exclusively due to the presence of the chromium complex and not to complexation of Zn^{2+} by the free ligand present in the medium, as observed for the transchelation experiment. Indeed, the same amounts of zinc and ligand were mixed with cytochrome *c* in the control experiment conducted in the absence of chromium complex. Thus, the effective redox potential for the Zn^{2+}/Zn couple should be strictly identical to that corresponding to the assay involving the chromium(III) complex. Furthermore, it is improbable that complexation of Zn^{2+} would significantly influence the reaction rate, as this should give rise to an induction period which is not observed in the present case, as no Zn^{2+} ions were present at the beginning of the reaction.

In our previous cytochrome *c* reduction studies involving the optically active $alamp^{2-}$ and $promp^{2-}$ complexes of cobalt(II)[11,38] and iron(II),[9] it was found that the reaction rate for the former is roughly 4 orders of magnitude slower than for the latter despite a slightly more negative redox potential of the Co^{III} vs Fe^{III} complexes. This rate difference has also been observed with the blue copper proteins plastocyanin and azurin and could be rationalized by the change of spin state in the case of cobalt(II).[10] As the experimental conditions used for the reaction with the chromium(II) complexes were different from those involving the iron(II) or cobalt(II) complexes, rate constants cannot be compared directly. Therefore, we attempt to discuss the initial rates under comparable conditions. At 25 °C and pH 7.5, initial cytochrome *c* and complex concentrations of 4×10^{-5} and 4×10^{-4} M, respectively, these initial rates are 6.7×10^{-6} M s^{-1} for [Fe^{II}((*S*,*S*)-promp] and 1.1×10^{-9} M s^{-1} for [Co^{II}((*S*,*S*)-promp)]. The measured initial rate for the reaction between cytochrome *c* and the electrochemically generated [Cr^{II}((*S*,*S*)-promp)] is 5×10^{-8} M s^{-1}. That means that the observed rate with the chromium(II) complex is about 2 orders of magnitude slower than the reaction with the corresponding iron(II) complex. Nevertheless, we must consider that the electrochemical reactions with the chromium(II) complexes take place exclusively inside the double layer at the surface of the electrode, whereas the reaction rates for chemical reduction correspond to bulk values. As the solution is vigorously stirred during the electrolysis, mass transfer can be neglected. If the thickness of the double layer is estimated to some 10 nm, the volume of the bulk solution would then be roughly 5×10^6 times that of the double layer. Taking into account the size of the solvated protein molecule, the presence of the positively charged chromium complex as well as the other electrolytes, the stationary concentration of the adsorbed protein in the double layer should be less than 20 times higher

(38) Scholten, U. Ph.D. Thesis, Université de Neuchâtel: Neuchâtel, Switzerland, 2005.

compared to the concentration in the solution (a complete coverage of the surface would result in a concentration of approximately 2×10^{-3} M). According to these assumptions, the estimated lower limit of the "real" reaction rate is 0.25 M s^{-1} with a second-order rate constant of about 8×10^6 M^{-1} s^{-1}.

Only a few kinetic studies of the reaction of cytochrome *c* with chromium(II) species have been published. A second-order rate constant value of 1.21×10^3 M^{-1} s^{-1} at pH 6.2 and 20 °C has been reported by Brittain et al.,[14] while Yandell et al. found a value of 3.1×10^3 M^{-1} s^{-1} at pH 7.0, $I = 1$ M NaCl, and 25 °C.[15] These authors studied also the influence of anions on the reaction rate. They observed a significant acceleration in the presence of coordinating anions such as Cl^- or SCN^-. This effect has been ascribed to a bridging mechanism in which the anion is forming a Fe−X−Cr intermediate, the anion replacing one of the iron−protein bonds. On the other hand, as cytochrome *c* carries a net positive charge at pH 7 due to the protonated lysine side chains, such a rate increase can also be due to electrostatic effects. Indeed, in a model system, we have shown that the rate of the electron transfer between a singly positively charged cobalt(III) complex and Fe^{2+} is increased by 4 to 5 orders of magnitude when the charge product of the reactants is changed from +2 to 0 upon complexation of Fe^{2+} by $alamp^{2-}$ or related ligands.[1] Assuming that a similar increase of the reaction rate could be induced by the complexation of Cr^{2+} by $promp^{2-}$ or $alamp^{2-}$, an effective rate constant of 10^6 to 10^7 M^{-1} s^{-1} for the reduction of cytochrome *c* with electrochemically generated chromium(II) complexes appears reasonable.

Conclusions

An extensive physicochemical characterization of optically pure chromium(III) complexes prepared from chiral pentadente pyridyldiaminocarboxylate ligands incorporating either two alanine ($alamp^{2-}$) or proline ($promp^{2-}$) residues is presented. Kinetic studies of both the zinc-mediated and electrochemical reduction of horse heart ferricytochrome *c* have evidenced a considerable acceleration by several orders of magnitude of the reduction rate when the chromium(III) complexes were added to the reaction mixture. This effect was best rationalized by assuming the in situ formation of transient labile chromium(II) species acting as an efficient electron-transfer catalyst. When these low-valent complexes are generated by amalgamated zinc powder, the redox potential of the Zn^{2+}/Zn couple is shifted toward more negative values due to zinc complex formation with the free ligand present in excess in the heterogeneous reaction mixture. The rate-determining step of cytochrome *c* reduction is most likely associated with the electron transfer rather than the formation of the chromium(II) species. Hence, the systems described herein should be suitable agents for unraveling stereoselectivity effects in the electron-transfer reaction. Compared to the results previously obtained for the corresponding cobalt(II) complexes,[11] these investigations could provide interesting information about the reactive site selected on the protein surface by these two metal ions. Indeed, the chromium(II) derivative, albeit less active than the $promp^{2-}$ complex of iron(II), was shown to more efficiently reduce cytochrome *c* than the corresponding cobalt(II) one. [Co^{II}(alamp)] is reputed to react stereospecifically according to an inner-sphere mechanism with the imidazole group of one solvent-exposed histidine residue located close to the heme edge (His-26 or His-33). Whether or not the divalent chromium complexes studied herein utilize the same electron-transfer path for reducing the iron center of the protein still remains an open question that should be answered by forthcoming investigations.

Acknowledgment. The authors express their gratitude to the following persons for their contribution to this work: Gilles Gasser, Thierry Vauthier, and Sabine Unternährer (Université de Neuchâtel); Jean-Nicolas Aebischer, Nicolas Charbonnet, Alexander Jungo, Gaël Pitarella, and Alexandre Vienne (Ecole d'Ingénieurs et d'Architectes de Fribourg); Inge Müller (Université de Fribourg); and Mélanie Bourdillon and Sophie Dal Molin (ICMUB). The Etat de Fribourg, the Etat de Neuchâtel, the Centre National de la Recherche Scientifique (CNRS), the Ministère de l'Enseignement Supérieur et de la Recherche, and the Conseil Régional de Bourgogne are thanked for having provided the infrastructure and some financial support.

Supporting Information Available: A partial view of the crystal packing of compound Λ-[Cr^{III}((*S*,*S*)-promp)H_2O]$ClO_4 \cdot 0.25H_2O$, cyclic voltammograms of Λ-[Cr^{III}((*S*,*S*)-promp)H_2O]ClO_4, Δ-[Cr^{III}-((*R*,*R*)-alamp)H_2O]ClO_4, and Λ-[Cr^{III}((*S*,*S*)-alamp)$(H_2O)_2$]ClO_4 as a function of the scan rate, visible absorption spectra recorded during the electrochemical reduction of cytochrome *c* in the presence of Λ-[Cr^{III}((*S*,*S*)-promp)H_2O]ClO_4, Δ-[Cr^{III}((*R*,*R*)-alamp)H_2O]ClO_4, and Λ-[Cr^{III}((*S*,*S*)-alamp)$(H_2O)_2$]ClO_4, and the crystallographic information file (CIF). This material is available free of charge via the Internet at http://pubs.acs.org.